UKACC International Conference on Control 2012
Cardiff, UK, 3-5 September 2012

Optimal Control for Mixing Enhancement in Boundary Layers at Membrane Walls

Hua Ouyang
School of Chemical Engineering
University of New South Wales
UNS Sydney, NSW 2052, Australia
Email: dr.hua.ouyang@gmail.com

Yuanqing Xia
School of Automation
Beijing Institute of Technology
Beijing 100081, China
Email: xia_yuanqing@bit.edu.cn

***Abstract*—This paper proposes a scheme for mixing enhancement in the boundary layers of pressure-driven membrane systems. This scheme uses an external electric field to activate the ions in the area adjacent to the membrane surface and generate an electro-osmotic flow. This scheme should reduce fouling and concentration polarization close to the membrane surface and may increase productivity of membrane systems. The objective of the feedback control design for this system needs to determine the voltage (and waveform) applied to the electrodes so that the electric field can effectively increase the mixing in the vicinity of membrane surface, while saving control power. This paper uses a mixing index in terms of the spatial gradients of the perturbation velocity field, which describes the mixing caused by both length stretching and folding. An optimal control problem is defined to maximize mixing in the area adjacent to the membrane and achieve control energy efficiency. In addition, the efficacy of the feedback scheme is validated by Computation Fluid Dynamics (CFD) simulation. The given control law not only solves the optimal problem but also provides the desired waveform for such applications.**

I. Introduction

Most solid surfaces in contact with water or an aqueous solution will be found to develop some type of electrical charge. The mechanisms that a surface acquires an electrical charge include preferential solution of surface ions, direct ionization of surface groups, substitution of surface ions, specific ion adsorption and so on [1]. The electrical charges gather on the solid surface and form an electric double layer. Physically, the two layers of ions align on the surface and lead to concentration polarization. In the membrane system in seawater filtration or brackish water filtration, the membrane can considered as a solid surface. Concentration polarization will result in fouling formed on the surface of the membrane.

Fouling and concentration polarization reduce the throughput and productivity of membrane systems and significantly increase operating costs. This in turn reduces the profitability of water treatment processes including desalination and recycling. Despite much work and improvement in the design and operation of membrane systems, throughput and productivity continue to be plagued by fouling and concentration polarization. Amongst the mechanisms that have been proposed to reduce fouling and concentration polarization, for example, feed pre-treatment [2], membrane surface modification or cleaning [3], reduction of solute concentration at the membrane surface by mixing enhancement in the flow offers the most promising way. Mixing enhancement in the vicinity of membrane surface can reduce concentration polarization in the region and hence lessen the chance of forming fouling. As a result, the throughput of membrane increases. This paper proposes a new approach to the reduction of solute concentration and fouling at the membrane surface based on producing electro-osmotic flow (EOF) instability.

Electric field is able to activate the ions in a solution to induce an electro-osmotic flow. This paper uses this fact to develop a new approach which enhances the mixing in the area adjacent to the membrane surface, via the use of electric field to generate an EOF in this area. Many results on using electric field to motivate electro-osmotic flows have been reported, for example, [4], [5], [6], [7], [8]. Distinct from most of these results which moves the ions in the whole channel like flow transport, the electric field in this scheme will mostly act on the boundary layer close to the membrane surface, where concentration polarization and fouling occur. This should enable us to use less energy to achieve mixing enhancement and hence it may be more energy efficient than existing electro-kinetic methods.

As mentioned in [9], mixing includes several types: the mixing of a single or similar fluids caused by stretching and folding of fluid; the mixing governed by diffusion and chemical reaction; the mixing caused by breakup and coalescence of fluid. Due to the variety of reasons leading to mixing, there are different mixing indices. Amongst these types, the mixing caused by fluid stretching and folding is the one of interest in the context of this paper. To describe this type of mixing, [9] gives a strict definition of stretching length based on the gradient of relative velocity, which is an important measure of mixing. Specifically, this stretching length uses the stretching tensor to describe mixing. Alexiadis et al [10] uses the vorticity or spin gradient tensor to describe the mixing induced by the vortices (folding) in the circumstance of membrane channel containing circular spacers. This paper adds up these two mixing measures and establishes a new mixing index.

In [11], [12], an objective function involving turbulent kinetic energy and a measure of the spatial gradients of turbulent velocities is used as the cost functional of an optimal flow control problem and maximizing this cost functional leads to mixing enhancement. This cost functional includes a Frobenius norm of the gradient of relative velocity (perturbation velocity). This term reflects the stretching of fluid elements explicitly but the folding measurement is implicit. This term is positively related to mixing but it is not proportional to that of enstrophy which is said to be more related to mixing. In this paper, we further explore the Frobenius norm of the gradient of perturbation velocity and use it as our new mixing index.

The mixing enhancement within the area adjacent to the membrane surface leads to the increase of the throughput of the membrane. This suggests that the mixing within this small vicinity is much more important than that in the bulk solution; i.e., the effect of the electric field will mostly apply to the boundary layer of the system. In this paper, we focus our attention on the mixing enhancement in this rectangular area. This requires us to relate the boundary control action to the mixing in this area. Gauss's divergence theorem states that the outward flux of a vector field through a closed surface is equal to the volume integral of the divergence of the region inside the surface[13]. Based on Gauss's divergence theorem, [11], [12] proposes a heuristic flow control methods which convert a mixing increase problem in a 3D pipe to a boundary control problem. This paper relates the electric field close to the membrane surface to the perturbation velocity and their spatial gradients inside the surface and hence transforms the problem into a boundary control problem.

In addition, the electric field used to activate the fluid flow in the vicinity is generated from a pair of electrodes, which are installed outside the membrane. This restricts us from manipulating the distributive value of electric field when we construct the feeding voltage. Once the electrodes are fixed, the spatial distribution of this electric field is fixed, viz., the voltage will not affect the shape of this distribution. This paper uses the integral of electric field strength on the membrane surface to construct the feedback control law. This makes the results of this paper distinct from those in [12], where distributive flow injection is used.

To improve the energy efficiency, we integrate the perturbation kinetic energy, the new mixing index and the control effort to define a cost functional and formulate an optimal problem for the fluid flow control problem for membrane systems. This requires that the control candidates solve such an optimal problem and maximize the cost functional. In addition, the efficacy of the proposed mixing enhancement scheme and the given control law has been validated by CFD simulations. CFD is a widely used tool for the studies of membrane system. This reliable tool is utilized in order to gain insight into the phenomena taking place inside membrane modules, to assist the design process and improve the performance of modules.

This paper is organized as follows: Section 2 presents a new mixing index and the theory of enhancing mixing in the area adjacent to the membrane surface. This section includes the main results of this paper. Sections 3 uses CFD simulations to illustrate the efficacy of the newly developed mixing enhancement scheme and the control law; Section 4 gives a brief conclusion to the paper. To simplify our presentation, the proof of the main result is given in the Appendix.

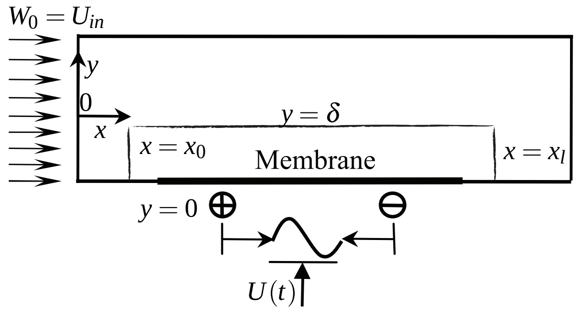

Fig. 1. The rectangular region close to the membrane surface.

II. Optimal Feedback Control for Mixing Enhancement in the Boundary Layer of Membrane System

In this section, a special scheme is developed, which uses an external electric field to stir up the flow in the area adjacent to the membrane surface and thereby increase the mixing in this area. As mentioned above, different from the previous methods which increase mixing in the whole channel [11], the new method restricts the influence of the external electric field in a region adjacent to the boundary layer. The electrodes are installed outside the membrane and the electric field does not activate the bulk flow in the channel. This reduces energy consumption and brings economic advantages to engineering practice.

As shown in Fig.I, the system we consider in this paper contains a rectangular channel, a piece of membrane installed on the bottom wall and a pair of electrodes. The electrodes are installed to generate the required voltage. An ions solution is fed into the channel from its inlet. The purpose of this research is to develop a control algorithm which generates the voltage signal (voltage and waveform) applied to the electrodes.

This study aims to enhance the mixing of fluid flow in area adjacent to the membrane surface and thereby reducing fouling and concentration polarization on the membrane. Because the purpose of this research is to explore the effect of the electric field on the flow in the area, it is reasonable to assume that the membrane is impermeable in our simulation study. We also assume that the bulk flow in the channel is a laminar flow. In addition, we use the velocity gradient $\frac{\partial w_x}{\partial y}$ on the membrane surface as the measurements of our system to be controlled.

In the channel, fluid flow satisfies the Navier-Stokes equation and the continuity equation

$$\frac{\partial \mathbf{W}}{\partial t} + (\mathbf{W}\cdot\nabla)\,\mathbf{W} = -\frac{1}{\rho}\nabla P + \frac{\mu}{\rho}\Delta\mathbf{W}, \tag{1}$$

$$\mathrm{div}(\mathbf{W}) = 0. \tag{2}$$

We assume that a velocity field $(\bar{\mathbf{W}}, \bar{P}) = (\bar{W}_x, \bar{W}_y, \bar{W}_z, \bar{P})$ is a steady state solution of the equations (1) and (2) corresponding to fully developed laminar flow in the channel. The solution to the equations (1) and (2) can be obtained analytically. For example, $(6U_{in}(1-\frac{y^2}{h^2}),0,12\mu U_{in}\frac{L-x}{h^2})$ is a solution for the system in our simulation. Here, U_{in} is the fluid velocity at the inlet of the channel, μ is the viscosity of the fluid, h and L are the height and the length of the channel. We can take these velocity components as the time-averaged values of the velocity field. Now, we define the perturbation variables

$$\mathbf{w} = (w_x, w_y, w_z) = \mathbf{W} - \bar{\mathbf{W}}, p = P - \bar{P}. \quad (3)$$

Substituting these variables into the equations (1) and (2), the Navier-Stokes equation and continuity equation become

$$\frac{\partial \mathbf{w}}{\partial t} + \left(\bar{\mathbf{W}}\cdot\nabla\right)\mathbf{w} + (\mathbf{w}\cdot\nabla)\bar{\mathbf{W}} + (\mathbf{w}\cdot\nabla)\mathbf{w} = -\frac{1}{\rho}\nabla p + \frac{\mu}{\rho}\Delta\mathbf{w}, \quad (4)$$

$$\operatorname{div}(\mathbf{w}) = 0. \quad (5)$$

in the domain $\Omega = \{(x,y,z) = [x_0, x_l] \times [-h/2, h/2]\}$ where $x_l - x_0$ is the length of the region we consider.

We define a rectangular prism $[x_0, x_l] \times [0, \delta]$, as shown in Fig. I, which contains all the flow being perturbed by the external electric field. Technically, it requires that the perturbation velocity components and the spatial gradients of the perturbation velocity field are all zeros on the surface $y = \delta$; i.e., the flow on and above this surface will not be perturbed by the electric field. Also, on the upstream and downstream sides of the rectangular prism, i.e., at $x = 0$ and $x = x_l$, the perturbation velocity components and the spatial gradients of the perturbation velocity field are also zero.

As the boundary condition on the membrane surface involves actuating the control law, it is worthy discussing the actuation scheme of the control at the first place. According to [5], [14], when an electric field is applied, the charges in the electric double layer induce fluid flow in the area adjacent to the membrane surface. As the boundary layer is very thin, the fluid flow on the membrane surface explains most effect of the electric field. Therefore, it is reasonable to assume that the external electric field only induces fluid flow on the membrane surface, rather than in y direction. The induced flow velocity is called slip velocity u_s and can be expressed as the product of electro-osmotic mobility μ_{EO} and the local electric field E as $\overrightarrow{u}_s = \mu_{EO}\overrightarrow{E} = \frac{\varepsilon\zeta}{\mu}\overrightarrow{E}$ where ζ is the zeta potential, ε is the permittivity, and μ is the viscosity of the fluid. In the context of this paper, the velocity $\overrightarrow{u}_s$ and the electric field $\overrightarrow{E}$ both take the x-axial direction as positive direction and the reverse direction as negative. Then, we write the slip velocity simply $u_s = \mu_{EO}E = \frac{\varepsilon\zeta}{\mu}E$. Therefore, the effect of the electric field on the fluid flow is transformed into a slip velocity on the membrane surface and the control problem becomes a boundary control problem.

Now, we can define the boundary condition for the equation (4). The equation (4) needs to satisfy the following boundary conditions on the rectangular prism $[x_0, x_l] \times [0, \delta]$

$x = x_0$: $w_x = 0$, $w_y = 0$, $\frac{\partial w_x}{\partial x} = 0$, $\frac{\partial w_x}{\partial y} = 0$, $\frac{\partial w_y}{\partial x} = 0$, $\frac{\partial w_y}{\partial y} = 0$;
$x = x_l$: ditto;
$y = \delta$: $w_x = 0$, $w_y = 0$, $\frac{\partial w_x}{\partial x} = 0$, $\frac{\partial w_x}{\partial y} = 0$, $\frac{\partial w_y}{\partial x} = 0$, $\frac{\partial w_y}{\partial y} = 0$;
$y = 0$: $w_x = u_s$, $w_y = 0$.

The boundary conditions on the surface $y = \delta$ are also the conditions for selecting δ.

In this section, we assume that the measurement of the system to be controlled, $\frac{\partial w_x}{\partial y}|_{y=0}$ is known for constructing feedback control signal.

To facilitate the development of the new mixing enhancement approach, we define two concepts: perturbation kinetic energy and mixing index. The perturbation kinetic energy, which is equivalent to the turbulent kinetic energy as defined in [11] when turbulence is the main cause of mixing, is defined as

$$E(\mathbf{w}) = \frac{1}{2}\int_\Omega |\mathbf{w}|^2 dV = \frac{1}{2}\int_{x_0}^{x_l}\int_0^\delta\int_0^{z_r}\left(w_x^2 + w_y^2 + w_z^2\right)dxdydz. \quad (6)$$

The mixing in this paper is defined as a measure of the spatial gradients of the perturbation velocity field:

$$M(\mathbf{w}) = \int_\Omega |\nabla\mathbf{w}|^2 = \int_\Omega \operatorname{Tr}\{\nabla\mathbf{w}^T\nabla\mathbf{w}\}dV. \quad (7)$$

Previously, Ottino [9] defined a stretching mixing rates as

$$\frac{dL}{dt} = \int_\Omega Tr\left(\Phi^T\Phi\right)dV, \quad (8)$$

where $\Phi = \frac{1}{2}\left(\nabla\mathbf{w} + (\nabla\mathbf{w})^T\right)$.

Defining $\Psi = \frac{1}{2}\left(\nabla\mathbf{w} - (\nabla\mathbf{w})^T\right)$, then, the mixing estimation parameter in [10], which mainly reflects the extent of mixing caused by vortices, can be rewritten in the following form

$$\frac{d\Lambda}{dt} = \int_\Omega Tr\left(\Psi^T\Psi\right)dV. \quad (9)$$

It is obvious that (7) is the sum of (8) and (9):

$$M(\mathbf{w}) = \int_\Omega |\nabla\mathbf{w}|^2 dV = \int_\Omega \operatorname{Tr}\left(\Phi^T\Phi\right)dV + \int_\Omega \operatorname{Tr}\left(\Psi^T\Psi\right)dV$$

That is, the mixing index (7) describes the mixing caused by both length stretching and folding induced by perturbations.

The proposed mixing enhancement scheme uses electric field to induce perturbations to the boundary layer. Fluid stretching and vortices account for most of the mixing caused by the perturbations. Therefore, the new mixing index can be used to describe the extent of the mixing caused by the perturbation in the circumstance of this paper. It is worth pointing out that this mixing index describes the mixing enhancement due to the perturbation caused by EOF and it does not reflect mixing inherent in the steady-state system and related to the original velocity gradients and momentum diffusion.

The control actuation of the proposed scheme is implemented through a pair of fixed electrodes and this gives the electric field a special distribution. This makes the proposed methods distinct from the flow control scheme in the literatures, for example, [12]. Based on aforementioned actuation mechanism, the slip velocity

$$u_s = U(t)f(x), \quad (10)$$

where $U(t)$ is the voltage applied to the electrodes, which is generated from our control algorithm, and

$$f(x) = C_1\left[\frac{x-l_1}{(x-l_1)^2+C_2} - \frac{x-l_2}{(x-l_2)^2+C_2}\right]$$

describes the distribution of the electric field with the parameters $C_1 = \frac{\varepsilon_w\zeta}{2\mu\ln\left(\frac{l_{i,2}-l_{i,1}-r_c}{r_c}\right)}$, and $C_2 = (h_m + r_c + \Delta y)^2$. Here, r_c is the radius of electrodes, h_m is the thickness of membrane and Δy is the distance between the electrode and the membrane outside. The other constants ε_w, ζ, μ are the permittivity, zeta potential, viscosity, respectively. Define $F = \int_0^{x_l} f^2(x)dx$, then

$$\begin{aligned}F &= \int_0^{x_l} C_1^2\left[\frac{x-l_1}{(x-l_1)^2+C_2} - \frac{x-l_2}{(x-l_2)^2+C_2}\right]^2 dx\\ &= C_1^2\int_0^{x_l}\left[\frac{x-l_1}{(x-l_1)^2+C_2}\right]^2 dx - 2C_1^2\int_0^{x_l}\frac{x-l_1}{(x-l_1)^2+C_2}\times\\ &\frac{x-l_2}{(x-l_2)^2+C_2}dx + C_1^2\int_0^{x_l}\left[\frac{x-l_2}{(x-l_2)^2+C_2}\right]^2 dx. \qquad (11)\end{aligned}$$

Now, we calculate the term on the right side of the equation (11) one by one. First we calculate the first term on the right side of (11). From the fact that $\left[\frac{x-l_1}{(x-l_1)^2+C_2}\right]^2 = \left[\frac{Ax+B}{(x-l_1)^2+C_2}\right]' + \left[\frac{Cx+D}{(x-l_1)^2+C_2}\right]$ where $A = -\frac{1}{2}$, $B = \frac{1}{2}l_1$, $C = 0$, $D = \frac{1}{2}$ and '′' means derivative, it follows that $\int_0^{x_l} C_1^2\left[\frac{x-l_1}{(x-l_1)^2+C_2}\right]^2 = \left[\frac{-1/2x+1/2}{(x-l_1)^2+C_2}\right]_0^{x_l} + \frac{1}{2\sqrt{C_2}}\arctan\frac{x}{2\sqrt{C_2}}\Big|_{-l_1}^{x_l-l_1} = -\frac{x_l-1}{2(x_l-l_1)^2+2C_2} - \frac{1}{2(l_1^2+C_2)} + \frac{1}{2\sqrt{C_2}}\arctan\frac{x_l-l_1}{2\sqrt{C_2}} - \frac{1}{2\sqrt{C_2}}\arctan\frac{-l_1}{2\sqrt{C_2}}$. In the same way, we have

$$\begin{aligned}&\int_0^{x_l}\left[\frac{x-l_2}{(x-l_2)^2+C_2}\right]^2 dx = \left[\frac{-1/2x+1/2}{(x-l_2)^2+C_2}\right]_0^{x_l}\\ &+\frac{1}{2\sqrt{C_2}}\arctan\frac{x}{2\sqrt{C_2}}\Big|_{-l_2}^{x_l-l_2}\\ &= -\frac{x_l-1}{2(x_l-l_2)^2+2C_2} - \frac{1}{2(l_2^2+C_2)} + \frac{1}{2\sqrt{C_2}}\arctan\frac{x_l-l_2}{2\sqrt{C_2}}\\ &-\frac{1}{2\sqrt{C_2}}\arctan\frac{-l_2}{2\sqrt{C_2}}.\end{aligned}$$

The second term on the right side of (11) $\frac{x-l_1}{(x-l_1)^2+C_2}\times\frac{x-l_2}{(x-l_2)^2+C_2} = \frac{Ax+B}{(x-l_1)^2+C_2} + \frac{Cx+D}{(x-l_2)^2+C_2}$ where $A = 0$ and B, C, D are the solution of the following linear equations

$$\begin{bmatrix}2(l_2-l_1) & 1 & 1\\ l_1^2-l_2^2 & -2l_2 & -2l_1\\ 0 & l_2^2+C_2 & l_1^2+C_2\end{bmatrix}\begin{bmatrix}C\\B\\D\end{bmatrix} = \begin{bmatrix}2\\-2(l_1+l_2)\\2l_1l_2\end{bmatrix}.$$

Then, we can calculate $\int_0^{x_l}\frac{x-l_1}{(x-l_1)^2+C_2}\times\frac{x-l_2}{(x-l_2)^2+C_2}dx = \frac{B}{\sqrt{C_2}}\arctan\frac{x}{2\sqrt{C_2}}\Big|_{-l_1}^{x_l-l_1} + C\frac{1}{2}\ln[(x-l_1)^2+C_2]_0^{x_l} + (D - Cl_2)\frac{1}{C_2}\arctan\frac{x}{2\sqrt{C_2}}\Big|_{-l_2}^{x_l-l_2}$ and thus F can be integrated analytically. From the above calculation, we can see that if the electrodes are installed, the distribution of the strength of the external electric field has been determined and F is a constant; i.e., the voltage is the only design variable of the electric field.

Now, we define the main problem to be solved in this section:

Problem A: The optimal feedback control problem is defined as finding an appropriate $U(t)$ for the control law $u_s(x,t) = U(t)f(x)$, to maximize the following cost functional

$$\begin{aligned}J(u) = \lim_{t\to\infty}\Bigg[&E(\mathbf{w}(t)) + \int_0^t\Bigg(\frac{\mu}{\rho}M(\mathbf{w}) + \Gamma(\mathbf{w}(t))\\ &-\alpha\int_{\bar{\Omega}}u_s^2(\tau)dA - \frac{\mu^2}{4\rho^2F\alpha}\left(\int_{\bar{\Omega}}f(x)\frac{\partial w_x}{\partial y}(\tau)dA\right)^2\Bigg)d\tau\Bigg].\end{aligned} \qquad (12)$$

where $\bar{\Omega}$ is the surface $y = 0$, and $\alpha > 0$ is a constant related to the amplitude of $U(t)$, which is used to adjust the applied voltage.

In the cost functional (12), the first term describes the perturbation kinetic energy of the flow; the second term is the mixing index; the third term describes the stretching caused by laminar flow and its definition is given in the Appendix The rest two terms will be explained in the following.

The following theorem gives a solution to Problem A:

Theorem 1: Given a constant $\alpha > 0$, the control law

$$U(t) = -\frac{\mu}{2\rho\alpha F}\int_{\bar{\Omega}}f(x)\frac{\partial w_x}{\partial y}dA \qquad (13)$$

solves Problem A. Also, the slip velocity

$$u_s(x,t) = -\frac{\mu}{2\rho\alpha F}f(x)\left(\int_{\bar{\Omega}}f(x)\frac{\partial w_x}{\partial y}\right)dA \qquad (14)$$

is the boundary condition on the lower wall of the channel in the system (4) and (5).

The proof of this theorem is given in the Appendix.

Here, $U(t)$ is a continuous signal. The amplitude of this voltage signal is $U_A = \|\frac{\mu\lambda}{2\rho}\left(\int_{\bar{\Omega}}f(x)\frac{\partial w_x}{\partial y}\right)/F\|$. Here, the formula of $U(t)$ is not an explicit function of time t but the system dynamics behind $\frac{\partial w_x}{\partial y}$ implies $U(t)$ is a function of t. The term $\frac{\partial w_x}{\partial y}$ itself is a function of time. In the area close to the membrane surface, the absolute perturbation velocity $|w_x|$ decreases in y direction and hence the sign $\frac{\partial w_x}{\partial y}$ is opposite to that of w_x. Since the output is fed back to the control input, the output penalty works in conjunction with the input penalty to minimize control effort.

III. Simulations and Mixing Measurements

In this section, the fluid dynamics of the EOF in a membrane system are simulated using ANSYS CFX to validate the efficacy of the control feedback approach; i.e., to test the effect of mixing enhancement in the vicinity of the membrane.

In the simulation, we consider the $2D$ case and use a channel with $L = 0.11$m and height $h = 0.004$m. The electrodes are cylindrical and $h_m = 0.00025$m, $r_c = 0.005$m. The distance between the two electrodes is 0.015m.

Because the purpose of the simulation is to validate the mixing enhancement in the area adjacent to the membrane surface when the electric field is applied, we assume that the membrane is impermeable. In our simulation, we also used the following parameters for the system: $h_m = 0.00025$m, $\mu = 0.001\text{kg}\cdot\text{m}^{-1}\cdot\text{s}^{-1}$, $\rho = 1000\text{kg}\cdot\text{m}^{-3}$, $\zeta = 0.02\text{kg}\cdot\text{m}^2\cdot\text{s}^{-3}\cdot\text{A}^{-1}$, $r_c = 0.005$m, $\varepsilon_w = 7.0832\times10^{-10}\text{m}^{-3}\cdot\text{kg}^{-1}\cdot\text{s}^4\cdot\text{A}^2$. The feeding flow velocity to the channel is a typical velocity in membrane systems used in water treatment, $\bar{W}_x = 0.14\text{m}\cdot\text{s}^{-1}$. In our simulation, the constant is selected as $\alpha = 0.008$, the Reynolds number of the flow is 280, and the step time is 10^{-5}s.

To give the system an initial perturbation, we first apply an oscillating voltage to the system, and then run the CFD simulation using the feedback control law given in this paper. The feedback is calculated using (13). As shown in Fig. 2, the simulation results show that the feedback oscillates around zero over time. The mixing extent caused by the electric field is measured by $M(\mathbf{w})$, which is the integral of spatial gradients of the perturbation velocity field over Ω. As the electric field is the only perturbation in the channel, Ω is selected as to contain all the perturbations in the channel. Fig. 3 shows the mixing effect of the mixing enhancement scheme, in comparison with case without electric field ($M(\mathbf{w}) = 0$). The mixing index has a scale of 10^{-6}) in Fig. 3. This is because the system itself has a scale of 10^{-6}. As shown in Fig. 3, the mixing index also has oscillating features and this shows that the mixing is caused by the input voltage. Therefore, this illustrates the efficacy of the proposed mixing enhancement scheme and control law.

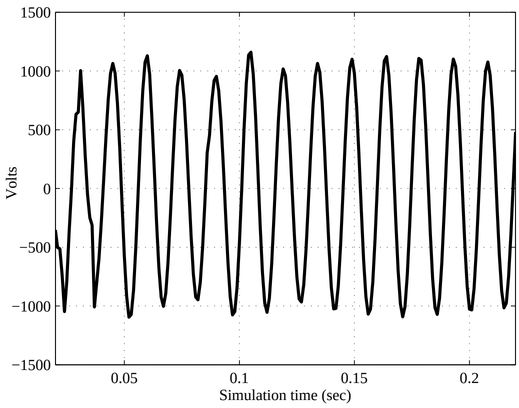

Fig. 2. The feedback control signal of the closed-loop system.

IV. Conclusion

This paper has proposed a method for mixing enhancement in the vicinity of the membrane surface and increasing the productivity of the membrane system. A new mixing index has been defined and incorporated into the cost functional of an optimal control problem. This paper uses the integral of an electric field distribution function to handle the actuation problem due to fixed electric field distribution and distributive slip velocity. An optimal control problem has been defined in this paper and the control law given in this paper solves this optimal problem and maximizes the cost functional. A

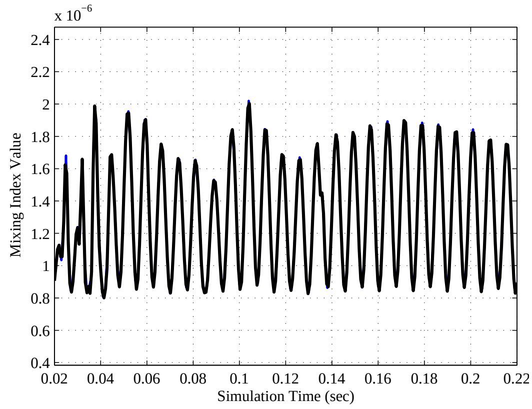

Fig. 3. The mixing index value when the control law (13) is applied to the system.

CFD simulation has been used to demonstrate the effect of the control law on mixing in the vicinity area adjacent to the membrane and has illustrated the efficacy of the proposed method. It also illustrates that the control law gives the desired waveform for such applications.

Appendix

A. Proof of Theorem 1:

The proof includes two parts: calculating the derivative of turbulent kinetic energy and verifying that the control maximizes the cost functional (12). We first consider the time derivative of the perturbation kinetic energy

$$
\begin{aligned}
\beta &= \frac{d}{dt}E(\mathbf{w}) = \int_\Omega \frac{\partial \mathbf{w}}{\partial t}\cdot \mathbf{w}dV \\
&= -\int_\Omega \left(\left(\bar{\mathbf{W}}\cdot\nabla\right)\mathbf{w} + (\mathbf{w}\cdot\nabla)\bar{\mathbf{W}}\right)\cdot\mathbf{w}dV - \int_\Omega (\mathbf{w}\cdot\nabla)\mathbf{w}\cdot\mathbf{w}dV \\
&\quad -\int_\Omega \frac{1}{\rho}\nabla p\cdot\mathbf{w}dV + \int_\Omega \frac{\mu}{\rho}\Delta\mathbf{w}\cdot\mathbf{w}dV.
\end{aligned} \tag{15}
$$

Now, we consider the terms on the right side one by one.

$$
\begin{aligned}
&-\int_\Omega (\mathbf{w}\cdot\nabla)\mathbf{w}\cdot\mathbf{w}dV = -\frac{1}{2}\int_\Omega \nabla(\mathbf{w}\cdot\mathbf{w})\mathbf{w}dV \\
&= -\frac{1}{2}\int_\Omega \operatorname{div}((\mathbf{w}\cdot\mathbf{w})\mathbf{w}) = -\frac{1}{2}\int_{\partial\Omega}[(\mathbf{w}\cdot\mathbf{w})\mathbf{w}]\cdot\mathbf{n}dA.
\end{aligned}
$$

On the surfaces $x = x_0, x = x_l$ and $y = \delta$, $\mathbf{w} = [w_x; w_y] = 0$. This results that $[(\mathbf{w}\cdot\mathbf{w})\mathbf{w}] = 0$. As $\mathbf{w}$ is perpendicular to $\mathbf{n}$ on the surface $y = 0$, the right side of the above equality is equal to zero. Therefore, $-\int_\Omega (\mathbf{w}\cdot\nabla)\mathbf{w}\cdot\mathbf{w}dV = 0$.

By the divergence theorem of Gauss, $-\frac{1}{\rho}\int_\Omega \nabla p\cdot\mathbf{w}dV = -\frac{1}{\rho}\int_\Omega \operatorname{div}(p\mathbf{w})dV = -\frac{1}{\rho}\int_{\partial\Omega} p\mathbf{w}\cdot\mathbf{n}dA$. As $\mathbf{w} = 0$ on the surfaces $x = x_0, x = x_l$ and $y = \delta$ and the fact that $\mathbf{w}\cdot\mathbf{n} = 0$ on the surface $y = 0$, we have $-\frac{1}{\rho}\int_\Omega \nabla p\cdot\mathbf{w}dV = 0$.

Consider the fourth term on the right side of (15). Using the Einstein summation notation, $\int_\Omega \frac{\mu}{\rho}\Delta\mathbf{w}\cdot\mathbf{w}dV = -2\nabla w_i\cdot\nabla w_i - w_i(\Delta w_i)]dV = \frac{\mu}{\rho}\int_\Omega \frac{1}{2}\Delta(w_i w_i)dV - \frac{\mu}{\rho}\int_\Omega |\nabla w|^2 dV$.

The term $\frac{1}{2}\frac{\mu}{\rho}\int_\Omega \Delta(w_i w_i)dV = \frac{1}{2}\frac{\mu}{\rho}\int_{\partial\Omega}(\nabla|\mathbf{w}|^2)\cdot\mathbf{n}dA$. On $\partial\Omega$, as $\mathbf{w} = 0$ on the surfaces $x = x_0, x = x_l$ and $y = \delta$, we only need to consider the surface $y=0$ where $\mathbf{n}=-j$. From the fact that $w_y|_{y=0}=0$, it follows that

$$\begin{aligned}\frac{1}{2}\frac{\mu}{\rho}\int_{\Omega}\Delta(w_i w_i)dV &= -\frac{1}{2}\frac{\mu}{\rho}\int_{0}^{z_r}\int_{x_0}^{x_l}2\left(w_x\frac{\partial w_x}{\partial y}+w_y\frac{\partial w_y}{\partial y}\right)_{y=0}dxdz\\ &= -\frac{\mu}{\rho}\int_{0}^{z_r}\int_{x_0}^{x_l}\left(w_x\frac{\partial w_x}{\partial y}\right)_{y=0}dxdz.\end{aligned}$$

Let $\Gamma=\int_{\Omega}((\bar{W}\cdot\nabla)w+(w\cdot\nabla)\bar{W})\cdot w dV$. Consider that $\bar{W}_y=\frac{\partial\bar{W}_y}{\partial y}=\frac{\partial\bar{W}_y}{\partial x}=0$ and our problem is two dimensional, we have

$$\Gamma(\mathbf{w})=\int_{\Omega}\left(\bar{W}_x\frac{\partial w_x}{\partial x}w_x+\bar{W}_x\frac{\partial w_y}{\partial x}w_y+w_y\frac{\partial\bar{W}_x}{\partial y}w_x\right)dV.$$

Then, we can conclude that

$$\frac{dE(\mathbf{w}(t))}{dt}=-\Gamma(\mathbf{w})-\frac{\mu}{\rho}\int_{0}^{z_r}\int_{0}^{l}w_x\frac{\partial w_x}{\partial y}|_{y=0}dxdz-\frac{\mu}{\rho}M(\mathbf{w}).$$

Now, we substitute this result into the cost functional (12) and prove that the control law (13) maximizes this cost functional.

$$\begin{aligned}\frac{1}{2}\frac{\mu}{\rho}\int_{\Omega}\Delta(w_i w_i)dV &= -\frac{1}{2}\frac{\mu}{\rho}\int_{0}^{z_r}\int_{x_0}^{x_l}2\left(w_x\frac{\partial w_x}{\partial y}+w_y\frac{\partial w_y}{\partial y}\right)_{y=0}dxdz\\ &= -\frac{\mu}{\rho}\int_{0}^{z_r}\int_{x_0}^{x_l}\left(w_x\frac{\partial w_x}{\partial y}\right)_{y=0}dxdz.\end{aligned}$$

Let $\Gamma=\int_{\Omega}((\bar{W}\cdot\nabla)w+(w\cdot\nabla)\bar{W})\cdot w dV$. Consider that $\bar{W}_y=\frac{\partial\bar{W}_y}{\partial y}=\frac{\partial\bar{W}_y}{\partial x}=0$ and our problem is two dimensional, we have

$$\Gamma(\mathbf{w})=\int_{\Omega}\left(\bar{W}_x\frac{\partial w_x}{\partial x}w_x+\bar{W}_x\frac{\partial w_y}{\partial x}w_y+w_y\frac{\partial\bar{W}_x}{\partial y}w_x\right)dV.$$

Then, we can conclude that

$$\frac{dE(\mathbf{w}(t))}{dt}=-\Gamma(\mathbf{w})-\frac{\mu}{\rho}\int_{0}^{z_r}\int_{0}^{l}w_x\frac{\partial w_x}{\partial y}|_{y=0}dxdz-\frac{\mu}{\rho}M(\mathbf{w}).$$

Now, we substitute this result into the cost functional (12) and prove that the control law (13) maximizes this cost functional.

$$\begin{aligned}J(u_s) &= \lim_{t\to\infty}\Bigg[E(\mathbf{w}(t))+\int_{0}^{t}\Bigg(-\frac{dE(\mathbf{w}(t))}{d\tau}-\Gamma(\mathbf{w}(t))\\ &\quad -\frac{\mu}{\rho}\int_{\bar{\Omega}}u_s\frac{\partial w_x}{\partial y}|_{y=0}dA+\Gamma(\mathbf{w}(t))-\alpha\int_{\bar{\Omega}}u_s^2(\tau)dA\\ &\quad -\frac{\mu^2}{4\rho^2F\alpha}\left(\int_{\bar{\Omega}}f(x)\frac{\partial w_x}{\partial y}(\tau)|_{y=0}dA\right)\Bigg)^2d\tau\Bigg]\\ &= E(\mathbf{w}(0))+\lim_{t\to\infty}\Bigg[\int_{0}^{t}\int_{\bar{\Omega}}\Bigg(-\frac{\mu}{\rho}u_s(\tau)\frac{\partial w_x}{\partial y}|_{y=0}dA\\ &\quad -\alpha\int_{\bar{\Omega}}u_s^2(\tau)dA\\ &\quad -\frac{\mu^2}{4\rho^2F\alpha}\left(\int_{\bar{\Omega}}f(x)\frac{\partial w_x}{\partial y}(\tau)|_{y=0}\right)dA\Bigg)^2d\tau\Bigg].\end{aligned}$$

Furthermore, we have

$$\begin{aligned}J(u_s) &= E(\mathbf{w}(0))+\lim_{t\to\infty}\Bigg[\int_{0}^{t}\Bigg(\frac{\mu}{\rho}\int_{\bar{\Omega}}-U(t)f(x)\frac{\partial w_x}{\partial y}|_{y=0}dA\\ &\quad -\alpha U(t)^2F-\frac{\mu^2}{4\rho^2F\alpha}\left(\int_{\bar{\Omega}}f(x)\frac{\partial w_x}{\partial y}(\tau)|_{y=0}dA\right)^2\Bigg)d\tau\Bigg]\\ &= E(\mathbf{w}(0))+\lim_{t\to\infty}\alpha F\int_{0}^{t}\Bigg[-\frac{U(t)}{\alpha F}\left(\frac{\mu}{\rho}\int_{\bar{\Omega}}f(x)\frac{\partial w_x}{\partial y}|_{y=0}\right)dA\\ &\quad -U(t)^2-\frac{\mu^2}{4\rho^2\alpha^2F^2}\left(\int_{\bar{\Omega}}f(x)\frac{\partial w_x}{\partial y}(\tau)|_{y=0}dA\right)^2\Bigg]d\tau\\ &= E(\mathbf{w}(0))\\ &\quad -\lim_{t\to\infty}F\int_{0}^{t}\left(U(t)+\frac{\mu}{\rho}\frac{1}{2\alpha F}\int_{\bar{\Omega}}f(x)\frac{\partial w_x}{\partial y}|_{y=0}dA\right)^2d\tau. \quad (16)\end{aligned}$$

When $U(t)=-\frac{\mu}{2\rho\alpha F}\int_{\bar{\Omega}}f(x)\frac{\partial w_x}{\partial y}|_{y=0}dA$, the integral in (16) is zero. Then, the maximum of (12) is achieved. Therefore, (14) holds. This completes the proof. □

References

[1] D. Myers, *Surfaces, interfaces, and colloids*. Wiley Online Library, 1999.

[2] M. Mänttäri, A. Pihlajamäki, E. Kaipainen, and M. Nyström, “Effect of temperature and membrane pre-treatment by pressure on the filtration properties of nanofiltration membranes,” *Desalination*, vol. 145, no. 1-3, pp. 81–86, 2002.

[3] H. Ma, C. Bowman, and R. Davis, “Membrane fouling reduction by backpulsing and surface modification,” *Journal of Membrane Science*, vol. 173, no. 2, pp. 191–200, 2000.

[4] S. Qian and H. Bau, “Theoretical investigation of electro-osmotic flows and chaotic stirring in rectangular cavities,” *Applied mathematical modelling*, vol. 29, no. 8, pp. 726–753, 2005.

[5] M. Oddy, J. Santiago, and J. Mikkelsen, “Electrokinetic instability micromixing,” *Analytical Chemistry*, vol. 73, no. 24, pp. 5822–5832, 2001.

[6] S. Shin, I. Kang, and Y. Cho, “Mixing enhancement by using electrokinetic instability under time-periodic electric field,” *Journal of Micromechanics and Microengineering*, vol. 15, p. 455, 2005.

[7] A. Rawool and S. Mitra, “Numerical simulation of electroosmotic effect in serpentine channels,” *Microfluidics and Nanofluidics*, vol. 2, no. 3, pp. 261–269, 2006.

[8] A. Stroock, M. Weck, D. Chiu, W. Huck, P. Kenis, R. Ismagilov, and G. Whitesides, “Patterning electro-osmotic flow with patterned surface charge,” *Physical review letters*, vol. 84, no. 15, pp. 3314–3317, 2000.

[9] J. Ottino, *The kinematics of mixing: stretching, chaos, and transport*. Cambridge Univ Pr, 1989, vol. 3.

[10] A. Alexiadis, D. Wiley, D. Fletcher, and J. Bao, “Laminar flow transitions in a 2d channel with circular spacers,” *Industrial & engineering chemistry research*, vol. 46, no. 16, pp. 5387–5396, 2007.

[11] O. Aamo and M. Krstić, *Flow control by feedback: stabilization and mixing*. Springer Verlag, 2003.

[12] A. Balogh, O. Aamo, and M. Krstic, “Optimal mixing enhancement in 3-d pipe flow,” *Control Systems Technology, IEEE Transactions on*, vol. 13, no. 1, pp. 27–41, 2005.

[13] M. R. Spiegel, *Schaum’s outline of theory and problems of vector analysis and an introduction to tensor analysis*. Schaum’s Outline Series, 1959.

[14] W. Wu, P. Selvaganapathy, and C. Ching, “Transport of particles and microorganisms in microfluidic channels using rectified ac electro-osmotic flow,” *Biomicrofluidics*, vol. 5, p. 013407, 2011.